Journal of Alloys and Compounds 509 (2011) 9377–9381

Contents lists available at ScienceDirect

Journal of Alloys and Compounds

journal homepage: www.elsevier.com/locate/jallcom

Effect of the impurity $Li_xNi_{1-x}O$ on the electrochemical properties of 5 V cathode material $LiNi_{0.5}Mn_{1.5}O_4$

G.Q. Liu [a,*], L. Wen [b], X. Wang [a], B.Y. Ma [a]

[a] School of Material and Metallurgy, Northeastern University, Shenyang 110819, China
[b] Chinese Acad Sci, Inst Met Res, Shenyang Natl Lab Mat Sci, Shenyang 110016, China

ARTICLE INFO

Article history:
Received 24 December 2010
Received in revised form 13 July 2011
Accepted 16 July 2011
Available online 22 July 2011

Keywords:
Lithium ion batteries
$LiNi_{0.5}Mn_{1.5}O_4$
Impurity $Li_xNi_{1-x}O$
Electrochemical properties

ABSTRACT

The formation of impurity $Li_xNi_{1-x}O$ when synthesizing spinel $LiNi_{0.5}Mn_{1.5}O_4$ using solid state reaction method, and its influence on the electrochemical properties of product $LiNi_{0.5}Mn_{1.5}O_4$ were studied. The secondary phase $Li_xNi_{1-x}O$ emerges at high temperature due to oxygen deficiency for $LiNi_{0.5}Mn_{1.5}O_4$ and partial reduction of Mn^{4+} to Mn^{3+} in $LiNi_{0.5}Mn_{1.5}O_4$. Annealing process can diminish oxygen deficiency and inhibit impurity $Li_xNi_{1-x}O$. The impurity reduces the specific capacity of product, but it does not have obvious negative effect on cycle performance of product. The capacity of $LiNi_{0.5}Mn_{1.5}O_4$ that contains $Li_xNi_{1-x}O$ can deliver about 120 mAh g^{-1}.

1. Introduction

In recent years, the 5 V cathode materials $LiNi_{0.5}Mn_{1.5}O_4$ for lithium ion batteries have attracted much attention. The high working voltage can lead to a high power density, so the batteries with this material as cathode will produce a high power output. So far, nearly all studies have focused on pure phase $LiNi_{0.5}Mn_{1.5}O_4$ and its derivatives, and great efforts have been made to avoid impurity phase such as $Li_xNi_{1-x}O$ [1–3]. It is generally believed that the impurity $Li_xNi_{1-x}O$ can deteriorate the electrochemical properties of products [4–6].The impurity $Li_xNi_{1-x}O$ results from oxygen deficiency in high temperature process of synthesizing $LiNi_{0.5}Mn_{1.5}O_4$ [7]. It is a common phenomenon that there is impurity $Li_xNi_{1-x}O$ in product when solid-state reaction method is used. Solid-state reaction is a commonly used method to prepare electrode materials for lithium ion batteries. It is simple and suitable for mass production. However, there is a trend that various wet chemical methods are employed to synthesize $LiNi_{0.5}Mn_{1.5}O_4$ in order to avoid impurity $Li_xNi_{1-x}O$ in products [8–10]. These wet chemical methods are more complicate and expensive to synthesize products than solid state reaction methods. If the impurity $Li_xNi_{1-x}O$ does not play a seriously negative role on products, the solid state methods should be recommended to produce $LiNi_{0.5}Mn_{1.5}O_4$ commercially.

It is necessary to study how the impurity $Li_xNi_{1-x}O$ affects the electrochemical performances of products. In this study, the spinel $LiNi_{0.5}Mn_{1.5}O_4$ compounds were synthesized by different solid state reaction methods. The products contained different amount of impurities. How the impurity $Li_xNi_{1-x}O$ affects the performance of products was studied and analyzed by electrochemical experiments such as galvanostatic measurements and cyclic voltametry.

2. Experimental

The spinel $LiNi_{0.5}Mn_{1.5}O_4$ compounds were synthesized by different solid state reaction methods. The chemical $Ni(OH)_2$, MnO_2 and $LiOH{\cdot}H_2O$ were used as starting materials. When synthesizing $LiNi_{0.5}Mn_{1.5}O_4$ (1), the molar ratio of Li:Ni:Mn was 1.02:0.5:1.5, and the reaction temperature was 850 °C for 12 h. The additional 2% of Li salt was to compensate for the loss of Li during high temperature reaction. When synthesizing $LiNi_{0.5}Mn_{1.5}O_4$ (2), the molar ratio of Li:Ni:Mn was 1.02:0.5:1.5. The reactants were calcined at 850 °C for 12 h and then annealed at 600 °C for 12 h.

The phase identification of the prepared samples was carried out by X-ray diffraction (XRD) using a Multiflex X-ray powder diffractometer (Rigaku Co. Ltd.). X-ray profiles were measured between 10 and 80° (2θ angle) with a monochromatic Cu Kα radiation source. Quantitative impurity phase analysis were made using Lutterotti' version of the Rietveld program MAUD [11]. The morphologies of the products were examined with a FEI NOVA NANOSEM430 scanning electron microscope (SEM).

The electrochemical properties of products were tested in cells with metallic lithium used as both negative and reference electrode. The cathode was separated from the Li anode by a layer of celgard 2300 membrane soaked with the electrolyte of 1 M $LiPF_6$ in a 1:1 (v/v) mixture of ethylene carbonate (EC) and dimethyl carbonate (DMC). The cathode was prepared by coating a slurry of 90% (weight percent) active material, 5% conducting carbon black, and 5% PVDF binder in NMP on an aluminum foil, drying in an oven, roller-pressing the dried coated foil, and punching out circular discs of 1.23 cm^2. The cells were assembled into CR2025 coin cells in an argon-filled dry box. Galvanostatic measurements were performed at a constant current density, in the range of 3.5–4.9 V. All the tests were carried out at room temperature. Cyclic voltametry (CV) was conducted at a scan rate of 0.1 mV s^{-1} between 3.5 V and 4.9 V versus Li/Li^+.

* Corresponding author. Tel.: +86 024 83673860; fax: +86 024 83687731.
E-mail address: liugq@smm.neu.edu.cn (G.Q. Liu).

0925-8388/$ – see front matter © 2011 Elsevier B.V. All rights reserved.
doi:10.1016/j.jallcom.2011.07.045

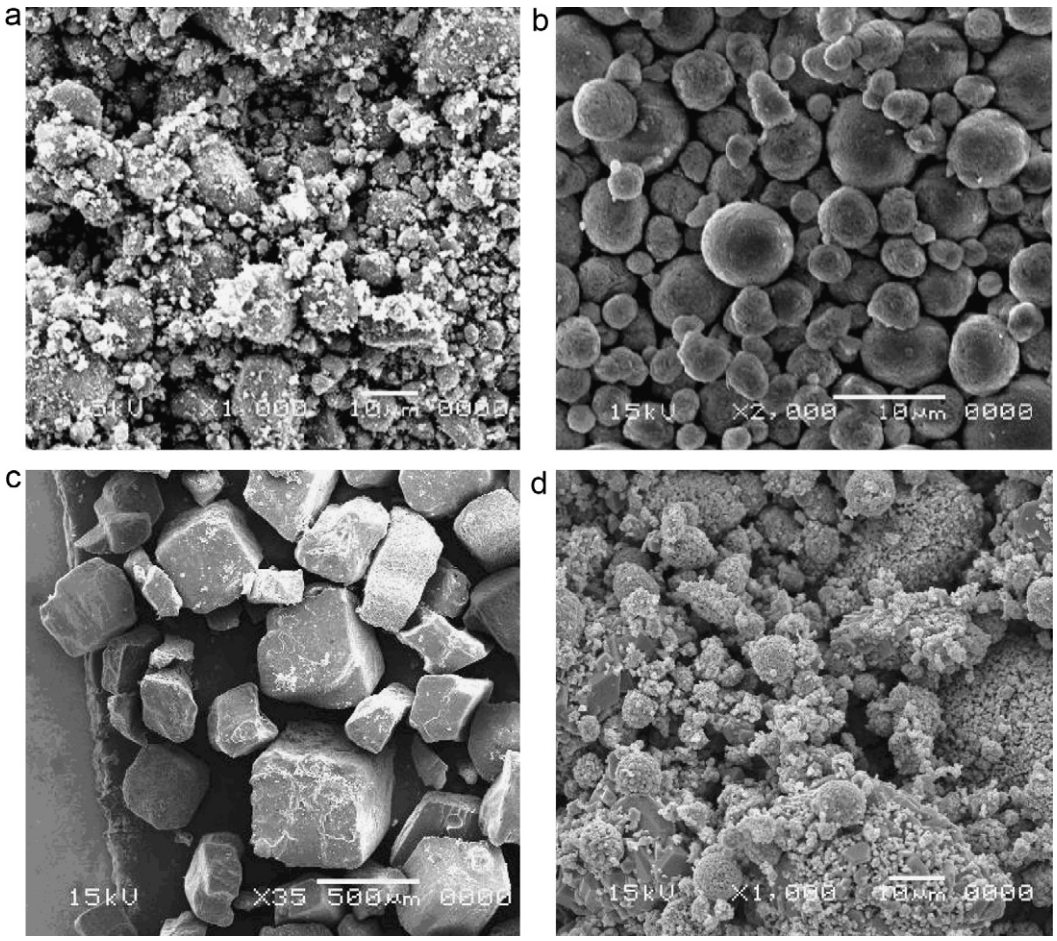

Fig. 1. Scanning electron micrograghs of reactants MnO_2 (a), $Ni(OH)_2$ (b), $LiOH{\cdot}H_2O$ (c) and product $LiNi_{0.5}Mn_{1.5}O_4$ (1).

3. Results and discussion

Fig. 1 shows the SEM images of reactant materials and product $LiNi_{0.5}Mn_{1.5}O_4$ (1). The micrograph of product is much different from those of reactants $Ni(OH)_2$ and $LiOH{\cdot}H_2O$, but somewhat like that of MnO_2.

Fig. 2 shows the XRD patterns of the prepared product $LiNi_{0.5}Mn_{1.5}O_4$ (1) and reference material $Li_{0.26}Ni_{0.72}O$. The $Li_{0.26}Ni_{0.72}O$ corresponds to the ICSD file No: 41890, with a space group of *Fd*3*m*. It can be seen that there are small peaks at 37.5°, 43.6° and 63.3° in the pattern of product, illustrating that there are secondary phases $Li_xNi_{1-x}O$. The arrows indicate these impurity peaks. The lattice parameter is calculated to be 8.201(7) Å.

The impurities $Li_xNi_{1-x}O$ have been reported in the previous literatures [12,13]. It is generally believed that this impurity can deteriorate the electrochemical properties. But its influence degree on the electrochemical properties of product has not been studied and explicitly reported so far. Fig. 3 shows the charge–discharge

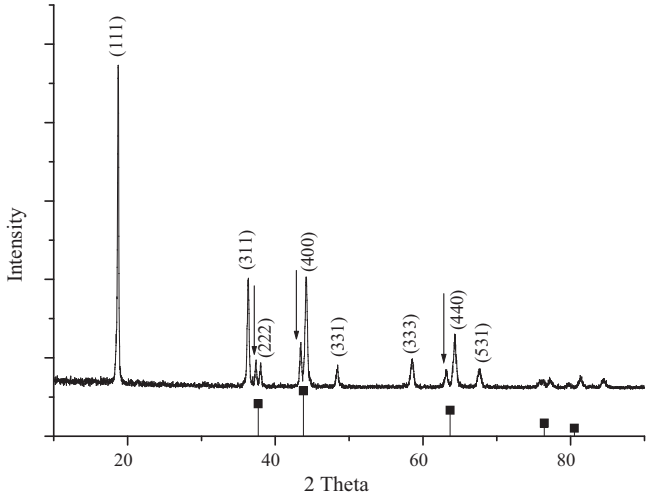

Fig. 2. XRD patterns of $LiNi_{0.5}Mn_{1.5}O_4$ (1) and $Li_xNi_{1-x}O$.

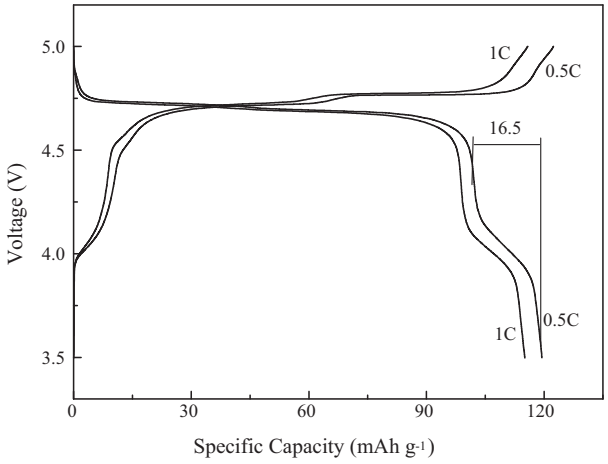

Fig. 3. Charge/discharge curves for $LiNi_{0.5}Mn_{1.5}O_4$ (1) at 0.5 C and 1.0 C.

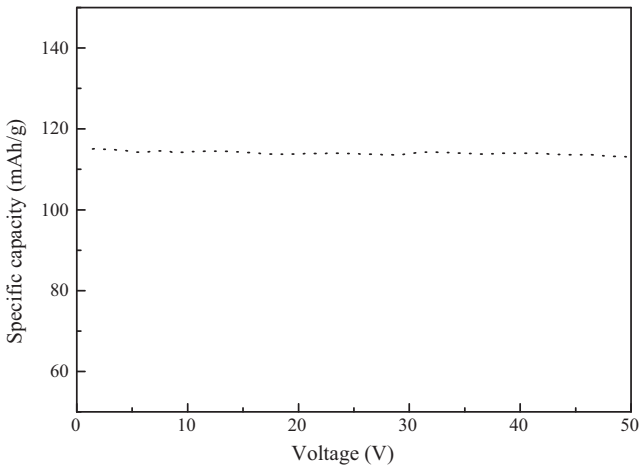

Fig. 4. Cycle performances of $LiNi_{0.5}Mn_{1.5}O_4$ (1).

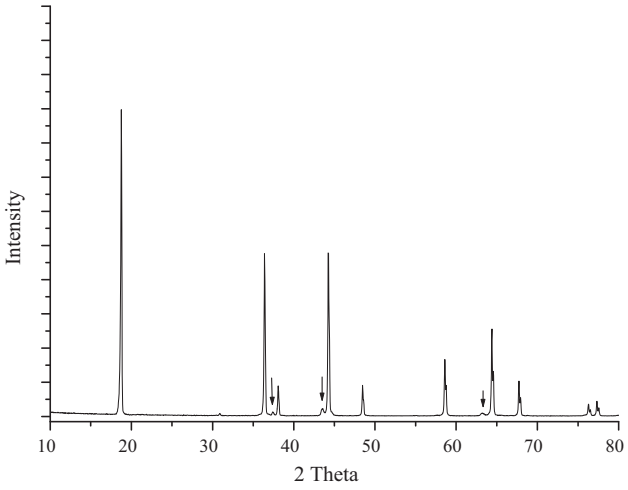

Fig. 6. XRD patterns of $LiNi_{0.5}Mn_{1.5}O_4$ (2).

curves of $LiNi_{0.5}Mn_{1.5}O_4$ (1) which contains impurity $Li_xNi_{1-x}O$. The discharge capacities are 118 mAh g^{-1} at 0.5 C and 115 mAh g^{-1} at 1.0 C, respectively. The cycle performance at 1.0 C is displayed in Fig. 4. It can be found that there is only small capacity decay after 50 cycles. The theoretical capacity of $LiNi_{0.5}Mn_{1.5}O_4$ is about 148 mAh g^{-1}. There is a capacity of about 26 mAh g^{-1} that is not delivered by sample $LiNi_{0.5}Mn_{1.5}O_4$ (1). It is reasonable to infer that a part of capacity loss results from the impurity $Li_xNi_{1-x}O$. However, it should also be found that the impurity $Li_xNi_{1-x}O$ does not deteriorate the cycle performances of product.

Fig. 5 shows the differential chronopotentiometry test result (dQ/dE). There are two oxidation peaks at 4.72 and 4.77 V and the corresponding reduction peaks at 4.68 and 4.71 V. This is an oxidation/reduction process of Ni^{2+}/Ni^{3+} and Ni^{3+}/Ni^{4+}. There is also a small peak at around 4.0 V, indicating that the oxidation/reduction process of Mn^{3+}/Mn^{4+} exits. The impurity $Li_xNi_{1-x}O$ and Mn^{3+} were resulted from oxygen deficiency in the synthesizing process. The reaction mechanism of synthesizing $LiNi_{0.5}Mn_{1.5}O_4$ can be denoted as the following equation: $0.5Ni(OH)_2 + 1.5MnO_2 + LiOH{\cdot}H_2O \rightarrow LiNi_{0.5}Mn_{1.5}O_4 + 2H_2O$

At high synthesizing temperature, $LiNi_{0.5}Mn_{1.5}O_4$ losses oxygen and disproportionates to a mixture of a spinel phase and a secondary phase $Li_xNi_{1-x}O$ because of partial reduction of Mn^{4+} to Mn^{3+}. This reaction process can be depicted as follows:

$$LiNi_{0.5}Mn_{1.5}O_4 qLi_zNi_{1-z}O + rLiNi_{0.5-w}Mn_{1.5+w}O_4 + sO_2$$

The oxygen deficiency for products will become more severe when the calcinations temperature is high.

In order to further investigate the influence of impurity $Li_xNi_{1-x}O$. The sample $LiNi_{0.5}Mn_{1.5}O_4$ (2) was also synthesized by another solid state reaction method. Fig. 6 shows the XRD pattern of product. The compound $LiNi_{0.5}Mn_{1.5}O_4$ (2) was synthesized at 850 °C for 12 h and then annealed at 600 °C for 12 h. It can be found that the intensity of impurity $Li_xNi_{1-x}O$ peaks decreased comparing to that of sample $LiNi_{0.5}Mn_{1.5}O_4$ (1). It is apparent that the annealing process diminishes the oxygen deficiency. There is no obvious difference between the diffraction angles of these two samples, which indicates that the lattice constants of the two samples are nearly the same. In fact, the lattice parameter of $LiNi_{0.5}Mn_{1.5}O_4$ (2) is calculated to be 8.192 (2) Å. The difference of lattice constant between the two samples is minute.

Fig. 7 illustrates the charge–discharge curves of the sample $LiNi_{0.5}Mn_{1.5}O_4$ (2). This test was conducted at 0.5 C charge current and different discharge current rates. The discharge capacities were 119.5 mAh g^{-1} at 0.5 C and 116.3 mAh g^{-1} at 1 C, respectively. The specific capacity in around 4 V was about 13.0 mAh g^{-1}. It is less than that of $LiNi_{0.5}Mn_{1.5}O_4$ (1). The specific capacity of sample $LiNi_{0.5}Mn_{1.5}O_4$ (1) in around 4 V was about 16.5 mAh g^{-1}. This proves that there was less amount of Mn^{3+} in sample $LiNi_{0.5}Mn_{1.5}O_4$ (2) than sample $LiNi_{0.5}Mn_{1.5}O_4$ (1). The reason is that there is less oxygen deficiency due to the annealing process.

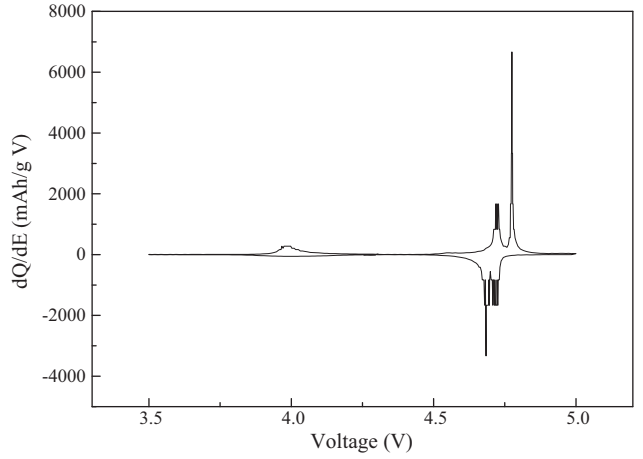

Fig. 5. Differential chronopotentiograms for $LiNi_{0.5}Mn_{1.5}O_4$ (1).

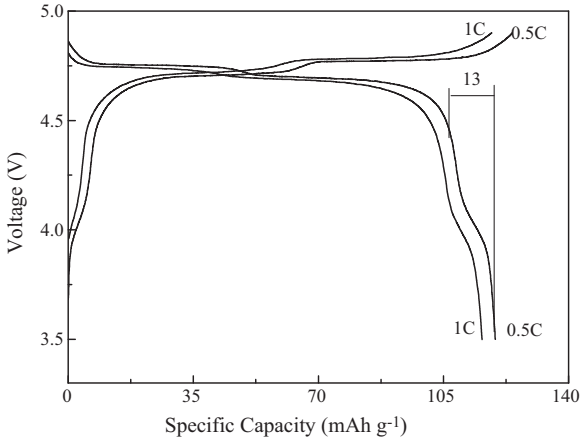

Fig. 7. Charge/discharge curves for $LiNi_{0.5}Mn_{1.5}O_4$ (2) at 0.5 C and 1.0 C.

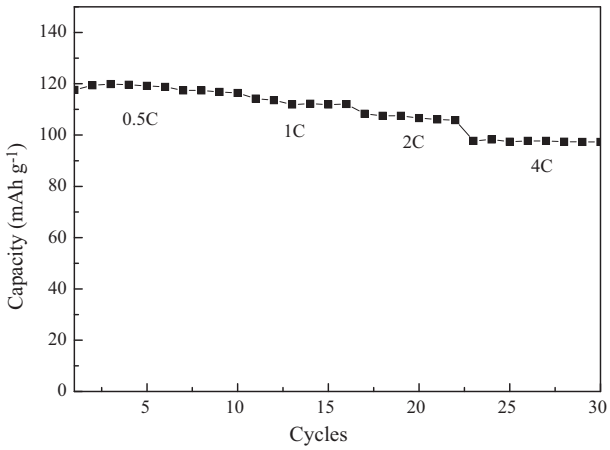

Fig. 8. Cycle performances of $LiNi_{0.5}Mn_{1.5}O_4$ (2).

The cycle performances of sample $LiNi_{0.5}Mn_{1.5}O_4$ (2) are shown in Fig. 8. Its discharge capacities at 2 C and 4 C were 107.5 and 98.5 mAh g^{-1}, respectively. The retaining rate of capacity was good for every current rate.

Fig. 9 shows the differential chronopotentiometry test result (dQ/dE) for sample $LiNi_{0.5}Mn_{1.5}O_4$ (2). There are two oxidation peaks at 4.71 and 4.77 V and the corresponding reduction peaks at 4.67 and 4.71 V. This is an oxidation/reduction process of Ni^{2+}/Ni^{3+} and Ni^{3+}/Ni^{4+}. There is also a small peak at around 4.0 V. Its intensity is weaker than that of sample $LiNi_{0.5}Mn_{1.5}O_4$ (1). This also indicates that the amount of Mn^{3+} in sample $LiNi_{0.5}Mn_{1.5}O_4$ (1) is less than that of $LiNi_{0.5}Mn_{1.5}O_4$ (1). The micrograph of sample is displayed in Fig. 10. Some polyhedrons appear in the SEM image. There is a broad distribution of particle size. Many small particles aggregate larger pellets. The largest single particle is about 20 μm.

Fig. 11 shows XRD refinement results of $LiNi_{0.5}Mn_{1.5}O_4$ (2). The observed data are indicated by crosses and the calculated profile is the continuous line overlaying them. The lower curve is the difference between the observed and calculated intensities at each step, plotted on the same scale and shifted a little downwards for clarity. The calculated pattern agrees quite well with the observed one. The phases analyses for the materials determined by Rietveld refinement are displayed in Table 1. From the above results, it can be seen that the $LiNi_{0.5}Mn_{1.5}O_4$ sample (2) possesses about 1.6% impurity content. In the same way, the $LiNi_{0.5}Mn_{1.5}O_4$ sample (1) possesses about 8.5% impurity content.

The above results demonstrate that the impurity $Li_xNi_{1-x}O$ can reduce the specific capacity of products. However, there is no obvious evidence that the impurity $Li_xNi_{1-x}O$ impairs the cycle performances of products. According the previous reports, the $Li_xNi_{1-x}O$ phase can be used as anode materials for lithium ion batteries, exhibiting good electrochemical properties. At 100 mA g^{-1}, its discharge capacity of the first cycle was up to 1480 mAh g^{-1} for $Li_{0.1}Ni_{0.9}O$ below 1.5 V [14]. Therefore, the impurity $Li_xNi_{1-x}O$ is not a complete insulator in the product. It is not an obstacle for lithium ion to transfer in the lattice of spinel $LiNi_{0.5}Mn_{1.5}O_4$.

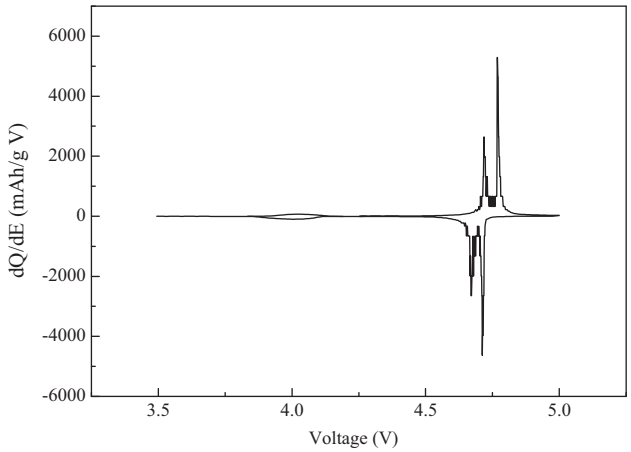

Fig. 9. Differential chronopotentiograms for $LiNi_{0.5}Mn_{1.5}O_4$ (2).

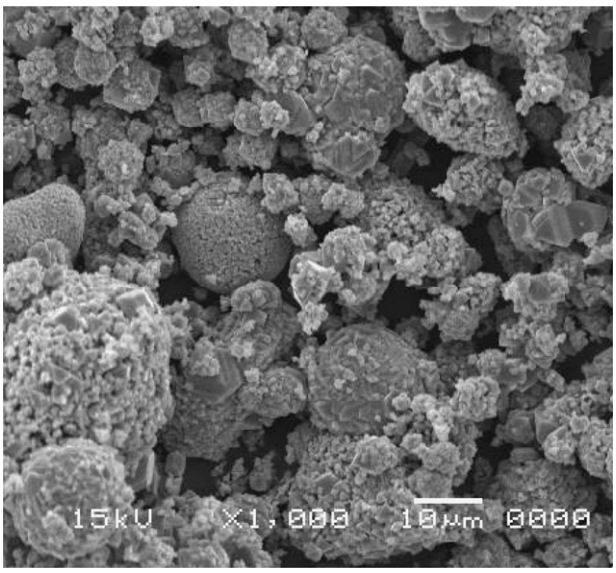

Fig. 10. Scanning electron micrographs of $LiNi_{0.5}Mn_{1.5}O_4$ (2).

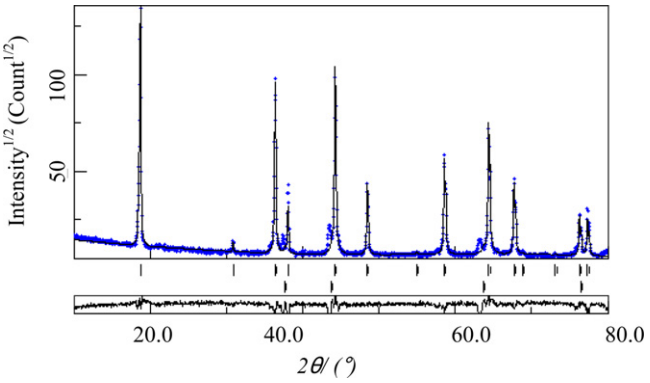

Fig. 11. XRD refinement results of $LiNi_{0.5}Mn_{1.5}O_4$ (2).

Table 1
Quantitative phase analysis results of $LiNi_{0.5}Mn_{1.5}O_4$ samples by Rietveld method.

	Content of $LiNi_{0.5}Mn_{1.5}O_4$ (wt%)	Content of $Li_{0.26}Ni_{0.72}O$ (wt%)	*R*wp(%)	*R*p(%)
Sample 1	98.4	1.6	12.1	7.2
Sample 2	91.5	8.5	11.6	6.8

4. Conclusions

The generation of impurity $Li_xNi_{1-x}O$ and its influence on properties of product $LiNi_{0.5}Mn_{1.5}O_4$ were studied. Producing $LiNi_{0.5}Mn_{1.5}O_4$ by solid state method usually accompanies the impurity $Li_xNi_{1-x}O$. At high synthesizing temperature, oxygen deficiency may take place for $LiNi_{0.5}Mn_{1.5}O_4$, resulting in secondary phase $Li_xNi_{1-x}O$ and partial reduction of Mn^{4+} to Mn^{3+}. An annealing process may inhibit the secondary phase $Li_xNi_{1-x}O$. The

impurity reduces the specific capacity of products, but it does not exert negative effects on cycle performance. The specific capacity of spinel $LiNi_{0.5}Mn_{1.5}O_4$ synthesized by solid state method is about 120 mAh g^{-1}.

Acknowledgement

This work was supported by the China Postdoctoral Science Foundation Project (20100471467).

References

[1] L.F. Xiao, Y.Q. Zhao, Y.Y. Yang, X.P. Ai, H.X. Yang, Y.L. Cao, J. Solid State Electrochem. 12 (2008) 687.
[2] H.S. Fang, Z.X. Wang, B. Zhang, X.H. Li, G.S. Li, Electrochem. Commun. 9 (2007) 1077.
[3] H.M. Wu, C.V. Rao, B. Rambabu, Mater. Chem. Phys. 116 (2009) 532.
[4] K. Amine, H. Tukamoto, H. Yasuda, Y. Fujita, J. Electrochem. Soc. 143 (1996) 1607.
[5] Q. Zhong, A. Bonakdarpour, M. Zhang, Y. Gao, J.R. Dahn, J. Electrochem. Soc. 144 (1997) 205.
[6] R. Alcaĭntara, M. Jaraba, P. Lavela, J.L. Tirado, Electrochim. Acta 47 (2002) 1829.
[7] A. Caballero, M. Cruz, L. Hernaĭn, M. Melero, J. Morales, E. Rodrıĭguez Castelloĭn, J. Electrochem. Soc. 152 (2005) A552.
[8] K. Takahashi, M. Saitoh, M. Sano, M. Fujita, K. Kifune, J. Electrochem. Soc. 151 (2004) A173.
[9] J.C. Arrebola, A. Caballero, L. Hernan, J. Morales, J. Power Sources 180 (2008) 852.
[10] M. Kunduraci, G.G. Amatucci, Electrochim. Acta 53 (2008) 4193.
[11] L. Lutterotti, S. Matthies, H.R. Wenk, A.J. Schultz, J. Richardson, J. Appl. Phys. 81 (1997) 594.
[12] S.H. Oh, S.H. Jeon, W. Il Cho, C.S. Kim, B.W. Cho, J. Alloy Compd. 452 (2008) 389.
[13] T.A. Arunkumar, A. Manthiram, Electrochim. Acta 50 (2005) 5568.
[14] Z.C. Li, C.W. Wang, X.L. Ma, L.J. Yuan, J.T. Sun, Mater. Chem. Phys. 91 (2005) 36.